A talin-dependent LFA-1 focal zone is formed by rapidly migrating T lymphocytes

Andrew Smith,[1] Yolanda R. Carrasco,[2] Paula Stanley,[1] Nelly Kieffer,[3] Facundo D. Batista,[2] and Nancy Hogg[1]

[1]Leukocyte Adhesion Laboratory and [2]Lymphocyte Interaction Laboratory, Cancer Research UK London Research Institute, London WC2A 3PX, England, UK
[3]Laboratoire de Biologie et Physiologie Intégrée, Université du Luxembourg, L-1511 Luxembourg, Luxembourg

Cells such as fibroblasts and endothelial cells migrate through the coordinated responses of discrete integrin-containing focal adhesions and complexes. In contrast, little is known about the organization of integrins on the highly motile T lymphocyte. We have investigated the distribution, activity, and cytoskeletal linkage of the integrin lymphocyte function associated antigen-1 (LFA-1) on human T lymphocytes migrating on endothelial cells and on ligand intercellular adhesion molecule-1 (ICAM-1). The pattern of total LFA-1 varies from low expression in the lamellipodia to high expression in the uropod. However, high affinity, clustered LFA-1 is restricted to a mid-cell zone that remains stable over time and over a range of ICAM-1 densities. Talin is essential for the stability and formation of the LFA-1 zone. Disruption of the talin–integrin link leads to loss of zone integrity and a substantial decrease in speed of migration on ICAM-1. This adhesive structure, which differs from the previously described integrin-containing attachments displayed by many other cell types, we have termed the "focal zone."

Introduction

The intrinsic ability of T lymphocytes (T cells) to migrate has been observed in vivo within lymph nodes and also in in vitro models of migration (Hogg et al., 2003; Miller et al., 2003; Mempel et al., 2004; Vicente-Manzanares and Sanchez-Madrid, 2004). T cells make use of the integrin lymphocyte function associated antigen-1 (LFA-1; αLβ2; CD11a/CD18) when migrating in response to chemoattractants either across the vasculature into lymph nodes or across stimulated vessels associated with infected tissue. The interaction with antigen-presenting cells is also a dynamic one in which the T cell crawls across the cell surface in an LFA-1–dependent manner, scanning for antigenic peptides. Thus, migration is a key aspect of T cell function and the integrin LFA-1 is implicated in this activity.

In vivo naive T cells within lymph nodes are able to migrate at speeds up to 40 μm/min (Miller et al., 2003; Mempel et al., 2004). Their frequent directional changes imply that this migration may be independent of gradients such as are generated by chemokines. Random migration can be modeled in vitro by direct activation of LFA-1 on T cells. This migration is regulated by myosin light chain activity that is controlled at the

leading edge by myosin light chain kinase and at the trailing edge by Rho kinase (ROCK; Smith et al., 2003). There is also regulation at the level of myosin IIA heavy chain as its phosphorylation inhibits migration (Jacobelli et al., 2004). Such findings suggest that integrins require linkage to the cytoskeleton in order to generate the force required for migration.

Although more than 20 proteins have been identified that bind to the cytoplasmic tails of integrins (Liu et al., 2000), accumulating evidence indicates that talin has a central role in both activating integrin and providing a cytoskeletal link (Calderwood and Ginsberg, 2003; Nayal et al., 2004; Tremuth et al., 2004). Talin is associated with LFA-1 in the peripheral supramolecular activation cluster of the immunological synapse (Kupfer and Singer, 1989; Monks et al., 1998) and, in neutrophils, talin and α-actinin bind sequentially to the β2 integrins during activation (Sampath et al., 1998). The talin head region contains a FERM (Band 4.1, ezrin, radixin, moesin) domain that activates β1, β2, and β3 integrins by binding to their β subunit cytoplasmic tails (Garcia-Alvarez et al., 2003; Kim et al., 2003). Phosphatidylinositol phosphate kinase type Iγ (PIPKIγ) also binds to the FERM domain, can compete with integrin for talin, and may have a role in turnover of adhesions (Di Paolo et al., 2002; Ling et al., 2002; Barsukov et al., 2003). For the migrating T cell, the connection between LFA-1 and the cytoskeleton has yet to be elucidated.

For cells such as fibroblasts, keratinocytes, and endothelial cells, migration proceeds through cycles of membrane protrusion

with new attachments at the leading edge followed by retraction at the trailing edge (Critchley, 2000; Webb et al., 2002; Wehrle-Haller and Imhof, 2002; Ridley et al., 2003). Such translocation occurs by the coordinated responses of rapidly turned over integrin-containing focal complexes (FC) at the front of the cell which evolve into the more substantial focal adhesions (FA) on the cell body and rear (Ballestrem et al., 2001; Laukaitis et al., 2001). However, neural crest cells and heart fibroblasts exhibit a form of integrin-mediated migration that is less dependent on the formation of FA/FC (Duband et al., 1988; Dunlevy and Couchman, 1993). Neural crest cells display an even distribution of β1 integrin and a migratory speed of ∼2 μm/min, which is greater than FA/FC-mediated movement (Duband et al., 1988; Strachan and Condic, 2003). On T cells, FC and FA are not observed and their greater speed and rapid alterations in direction distinguishes their form of cell movement from those cells that chiefly use FA/FC.

It is therefore of interest to investigate how T cells control LFA-1 distribution and activity while undergoing migration on intercellular adhesion molecule-1 (ICAM-1). We identify a structure comprising a zone of high affinity LFA-1 that is restricted to the mid-cell area and is dependent on talin. The disruption of this structure, or failure to form, results in the loss of T cell migratory activity.

Results

Migration of T cells on ICAM-1–expressing target cells

To understand the role of LFA-1 in T cell migration, we activated LFA-1 directly with Mg^{2+} and followed the random migration of the cells on a monolayer of ICAM-1–expressing human umbilical vein endothelial cells (HUVECs). At the HUVEC interface, T cell LFA-1 displayed a heterogeneous distribution with low levels in the lamellipodia and a concentrated area corresponding to the mid-region of the cell (Fig. 1, A and B). The uropod at the rear of the cell formed an elevated nonadherent cell protrusion that made minimal contact with the HUVECs. The distribution of LFA-1 at the interface remained constant as the cells migrated (Video 1, available at http://www.jcb.org/cgi/content/full/jcb.200412032/DC1). The addition of function blocking anti–LFA-1 (mAb 38) resulted in the loss of LFA-1 redistribution to the mid-cell region and reduced adhesion to the HUVECs (unpublished data).

A second model of migration, making use of ICAM-1-GFP–expressing COS cells, allowed us to investigate LFA-1–ICAM-1 interactions. T cells migrating across the COS cells displayed a skewed pattern of LFA-1 expression similar to that seen on HUVECs (Fig. 1 C, a and c, red). However the bound ICAM-1 was concentrated in a restricted region corresponding to the mid-cell area of the migrating T cell (Fig. 1 C, b and c, green). The merged image revealed the overlap between LFA-1 and ICAM-1 (Fig. 1 C, c, yellow). The uropod expressed a high LFA-1 level but did not show concentrated ICAM-1. Therefore, the ability to concentrate ICAM-1 was restricted to a distinct area on the migrating T cell. Quantitation of the ICAM-1 levels in the mid-cell compared with the lamellar region re-
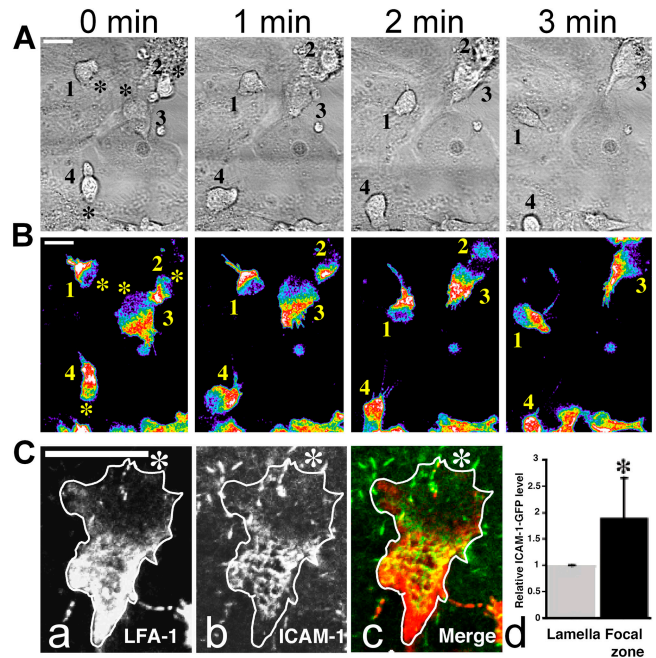

Figure 1. **Confocal image of a T cell migrating in the presence of 5 mM $MgCl_2$ on a target cell expressing ICAM-1.** T cells labeled with Alexa 488 nonblocking anti–LFA-1 Fabs and migrating on TNF-α–activated HUVECs. (A) Phase images of the pattern of migration of four T cells (1–4) over 3 min. (B) False color images of the same four T cells showing expression levels of LFA-1 (highest [white] to lowest [blue]). The asterisk denotes the leading edge of each cell. (C) T cell (white outline) migrating on ICAM-1–transfected COS-7 cells (the asterisk denotes the T cell leading edge). (a) T cell labeled with anti–LFA-1 mAb (red). (b) COS-7 cells expressing ICAM-1-GFP (green). (c) Merge of the two images in panels a and b. Colocalization of LFA-1 and ICAM-1 can be observed in the mid-cell region. All images were taken with a 63× oil immersion objective. Bars, 10 μm. (d) Quantitation of ICAM-1 density in focal zone (black bar) compared with lamellar region (gray bar) on migrating T cells (n = 9; ±SD). *, P < 0.001.

vealed an approximately twofold increase (Fig. 1 C, d). Finally, T cells moving on ICAM-1 toward the chemotactic stimulus SDF-1(CXCL12) also demonstrated an LFA-1 pattern identical to that observed upon migration on HUVECs (Fig. S1, available at http://www.jcb.org/cgi/content/full/jcb.200412032/DC1). Thus, T cells contain a distinctive region of concentrated and ligand-bound LFA-1 when migrating on target cells. This migratory structure is substantially different from the multiple FCs and FAs that have been described for other cell types and constitutes an integrin-containing complex that we have termed the "focal zone."

Zone of active LFA-1: a novel ICAM-1 binding structure

To analyze LFA-1–ICAM-1 with minimal interference from other receptor pairs, we next investigated T cell migration on glycophosphoinositide-linked ICAM-1 incorporated into planar lipid bilayers (Dustin et al., 1997; Carrasco et al., 2004). In addition, this model permitted more detailed visualization of contact between ligand and receptor. In this setting, the striking feature of T cells was the formation of a single mid-cell region of concentrated ICAM-1 corresponding to the focal zone associated with T cells migrating on target cells (Fig. 2 A and
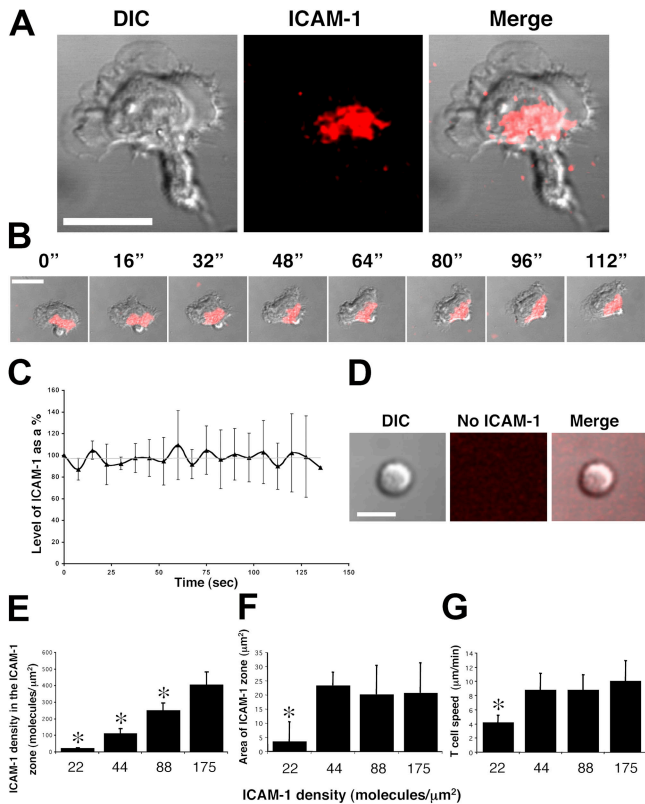
A DIC | ICAM-1 | Merge

B 0" 16" 32" 48" 64" 80" 96" 112"

C

D DIC | No ICAM-1 | Merge

E **F** **G**

Figure 2. **Structure and stability of the ICAM-1 binding zone on migrating T cells.** Human T cells were added to ICAM-1–containing planar lipid bilayers (175 molecules/μm^2) in the presence of 5 mM MgCl$_2$ at 37°C. (A) The location of a concentrated zone of ICAM-1 (red) on a migrating T cell. (B) A T cell migrating over time displays the stability of the zone of ICAM-1 binding in relation to its intensity and cellular position. (C) The total amount of ICAM-1 within the zone of migrating T cells was calculated at time 0 (equals 100%) and the relative ICAM-1 levels were recorded at intervals over a period of 130 s. All results are expressed as an average of 10 cells ± SD. (D) The lack of ICAM-1 incorporation in the bilayer resulted in the failure of T cell attachment and polarization. Bars, 10 μm. (E) The density of ICAM-1 in the zone decreases as the ICAM-1 level in the lipid bilayer decreases (r^2 = 0.9677). (F) The area occupied by the zone of ICAM-1 shows stability over a range of ICAM-1 concentrations (175 to 44 molecules/μm^2) and then declines by 22 molecules/μm^2. (G) The migration speed is constant between 175 and 44 molecules/μm^2 and reduces significantly (P < 0.01) below this level. E–G were composed from values obtained from the same experiments (n = 5–7; ±SD). All images were taken with a 63× oil immersion objective. *, P < 0.01.

Video 2, available at http://www.jcb.org/cgi/content/full/jcb.200412032/DC1). Observation over time showed that the zone maintained a constant cellular location (Fig. 2 B), and quantification of the density of ICAM-1 indicated that it also remained stable over time at $\sim$400 molecules/μm^2 (Fig. 2 C). The process was totally ICAM-1 dependent, as the T cells failed to either attach or migrate in its absence (Fig. 2 D).

A decreasing density of ICAM-1 in the bilayer correlated with diminished ICAM-1 density associated with the T cell (r^2 = 0.9677; Fig. 2 E). In spite of the loss in ICAM-1 density, the zone sustained a constant area (21 μm^2; Fig. 2 F) and the migratory speed remained stable at 9.2 ± 3.4 μm/min between 44–175 ICAM-1 molecules/μm^2 (Fig. 2 G). However, at <44 molecules/μm^2, the zone was no longer detectable and a decrease in speed of migration was observed. The findings suggest that a minimum density of ICAM-1 is necessary for opti-

mal speed and that this is coincident with the formation of the zone. In contrast, exposure to higher ICAM-1 levels in the bilayer has little impact on the area of the zone or T cell speed. This could be due to constraints on the migratory machinery or an optimal rate having been achieved through limitations of other molecular interactions.

## Membrane distribution of LFA-1 on the migrating T cell

To investigate total LFA-1 expression, we stained migrating T cells with Alexa 488–conjugated nonblocking anti–LFA-1 Fab′ fragments as in Fig. 1 A. The distribution of LFA-1 was found to be substantially increased in two cellular locations: toward the mid-cell region, where it overlapped with the high levels of ICAM-1 in the focal zone, and in the uropod, where concentrated ICAM-1 was not observed (Fig. 3 A). Serial sections through a migrating T cell revealed that although LFA-1 was concentrated at the level of the bilayer, it also surrounded the entire surface of the cell with high levels in the uropod (Fig. 3 B). This distinctive pattern of LFA-1 distribution is in contrast to other membrane proteins such as CD3, which is evenly expressed over the entire membrane, as well as CD43 and ICAM-3, which are concentrated in the uropod (Fig. S2, available at http://www.jcb.org/cgi/content/full/jcb.200412032/DC1).

To investigate how LFA-1 becomes redistributed after ICAM-1 engagement, we recorded the initial contact between T cells and the bilayer. At 30 s the T cell displayed a centralized point of attachment to ICAM-1 (Fig. 3 C). As the T cell spread and began to polarize (30 to 60 s), LFA-1 levels increased at the edge furthest from the lamellipodia and the area of concentrated ICAM-1 enlarged. As the T cell started to translocate (60 to 90 s), the greatest proportion of LFA-1 was associated with the mid-cell and uropod regions. In fully migratory T cells, there was an approximately five- and eightfold increase of LFA-1 in the focal zone and the uropod, respectively (Fig. 3 C, green image and trace), compared with the level in the lamellipodia. When the intensity of the concentrated ICAM-1 was quantified from the initiation of contact to time of migration, its level remained constant (Fig. 3 C, red image and trace). These findings demonstrate that the formation of the focal zone and LFA-1 redistribution occur in association with T cell polarization and spreading (Video 3, available at http://www.jcb.org/cgi/content/full/jcb.200412032/DC1).

T cell contact with ICAM-1 extends beyond the focal zone

The focal zone is an area of direct contact between LFA-1 and ICAM-1, but it is also possible that ligand engagement occurs in other areas of the cell. To further examine the contacts between T cell LFA-1 and ICAM-1, we used the lipid bilayer model together with interference reflection microscopy (IRM). The IRM images revealed a pattern of intermittent contact in the lamellipodial area (Fig. 4 A, black arrow), whereas the mid-cell region displayed uniformly dense contact with ICAM-1 (IRM; Fig. 4 A, double arrow), indicating that this region was the most firmly attached area of the cell. This latter area was coincident with the focal zone (Fig. 4 A, ICAM-1 and merge)

Figure 3. **LFA-1 surface distribution on T cells migrating on ICAM-1.** Alexa 488–labeled nonfunctional blocking anti–LFA-1 Fab′ is used to identify surface distribution of LFA-1 without cross-linking or affecting ICAM-1 binding activity. (A) Distribution of ICAM-1 (red) and LFA-1 (green) on a migrating T cell at the lipid bilayer level. The merge image demonstrates colocalization of LFA-1 and ICAM-1 in the mid-cell region. (B) Confocal z-stack (each slice = 1 μm) through a T cell migrating on ICAM-1. LFA-1 (green) is most intense at the level of the lipid bilayer in the mid-cell region, with weak expression in the lamellipodia. LFA-1 is visible over the entire surface, with a pattern of increased intensity toward the trailing edge and the uropod. (C) Distribution of LFA-1 (green) and concentrated ICAM-1 (red) was recorded over 180 s after initial contact with ICAM-1 in the lipid bilayer. The top panels show DIC images of a T cell polarizing and migrating. The bottom image panels illustrate the merged LFA-1 and ICAM-1 signals. The arrows (Merge) are split into red (bilayer only) and black (cell and bilayer) and show the regions where the profile data (bottom) was calculated. The arrow tip is located at the trailing edge. The graphs depict the fold increase of LFA-1 compared with the single plasma membrane level in the lamellipodia (green) and ICAM-1 compared with the bilayer level (red) over the entire T cell between 30–180 s after initial contact. All images were taken with 63× oil immersion objective. Bars, 10 μm.
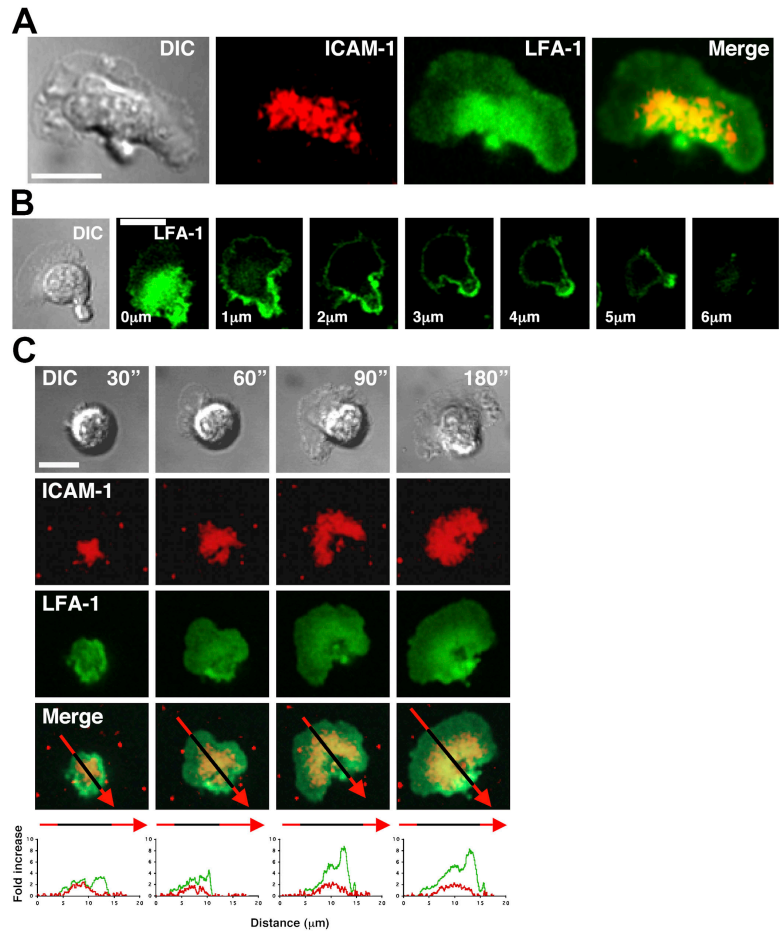
and comprised 22% (equal to 20.7 μm²) of the total area in contact with the bilayer (Fig. 4 B). Our findings show that the lamellipodia region provides adhesive interactions between LFA-1 and ICAM-1, but these interactions do not result in an accumulation of ICAM-1 that is distinguishable from the level in the lipid bilayer. Therefore, as the total area making adhesive contact was greater than the focal zone, attachment to ICAM-1 must be mediated by distinct membrane distributions of LFA-1, potentially in different activity states. Finally, although expressing high levels of LFA-1, the uropod was IRM negative, indicating a lack of interaction with ICAM-1 (Fig. 4 A, white arrow). Despite the focal zone and uropod containing high levels of LFA-1, the lack of ICAM-1 binding activity in the uropod indicates differential control of integrin activity between these two cellular locations.

High affinity LFA-1 is restricted to the focal zone

Next, we wanted to explore the activation status of LFA-1 on the migrating T cell. To locate LFA-1 in the high affinity conformation, we used Fab′ fragments of mAb 24, which selectively recognizes high affinity LFA-1 (Dransfield and Hogg, 1989; Hogg et al., 2002). When added to migrating T cells, mAb 24 immediately localized to the focal zone (Fig. 5 A, compare ICAM-1 [red] with mAb 24 [green]), providing evidence that this region contained high affinity LFA-1. Localiza-

tion of high affinity LFA-1 to the focal zone was also a feature of T cells migrating on target cells expressing ICAM-1-GFP (Fig. 5 B). In contrast, no mAb 24 binding was displayed by the uropod (Fig. 5 A, DIC) nor was it detectable in the lamellipodia, even after long exposures to this mAb (Fig. S3, available
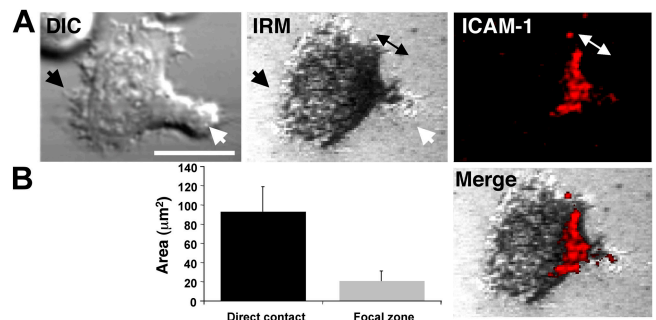
Figure 4. **IRM reveals the areas of direct contact between migrating T cells and ICAM-1.** (A) The DIC image compared with the IRM image and the ICAM-1 binding focal zone (red). The IRM image identifies the total area of the T cell in direct contact with ICAM-1 in the bilayer and demonstrates intermittent, close, and lack of attachments in lamellipodia, focal zone, and uropod, respectively. Double-sided arrow, closest attachment to the substrate; black arrow, the leading edge; white arrow, the uropod of the migrating T cell. Overlaying the ICAM-1 and IRM images shows that the area of uniform attachment colocalizes with the focal zone. (B) Quantification of the area in contact with the bilayer compared with the area of the focal zone (n = 10; ±SD). All images were taken with a 63× oil immersion objective. Bars, 10 μm.
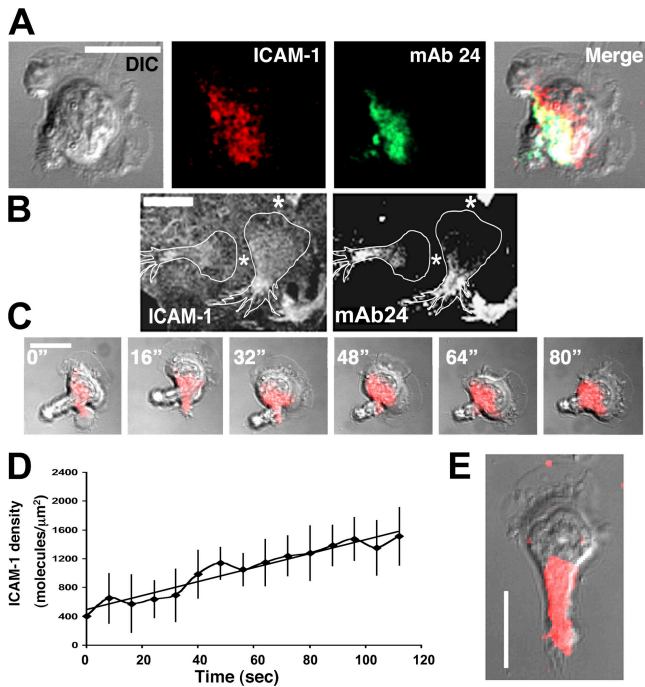
Figure 5. **The location of high affinity LFA-1 on T cells migrating on ICAM-1.** (A) A T cell migrating on ICAM-1 (red) and labeled with mAb 24 Fab' (green) showing the distribution of the high affinity LFA-1. The merged image shows the colocalization of mAb 24–bound LFA-1 with the ICAM-1 within the focal zone. (B) T cells (white outline; asterisk denotes the leading edge) migrating on ICAM-1-GFP–transfected COS-7 cells in the presence of Alexa 546 Fab' of mAb 24 (10 μg/ml) for 120 s before fixation. (C) A T cell migrating on ICAM-1 after the addition of mAb 24 at 0 s shows a build up of ICAM-1 restricted to the focal zone over 80 s. (D) Quantification of the ICAM-1 build up after mAb 24 addition reveals a linear relationship over 112 s ($r^2 = 0.93$), resulting in the ICAM-1 density rising from ~400 to ~1,500 molecules/μm^2, equating to ~10 molecules/μm^2/s ($n = 5$; ±SD). (E) Prolonged exposure to mAb 24 (>300 s) results in the extension of the focal zone into the uropod and an elongated morphology. In comparison, the ICAM-1 levels within the lamellipodia remain the same as in the bilayer. All images were taken with a 63× oil immersion objective. Bars, 10 μm.

at http://www.jcb.org/cgi/content/full/jcb.200412032/DC1). Therefore, it is likely that the leading edge adhesions and uropod do not involve high affinity LFA-1 or at least only at very low levels.

The high affinity conformation of LFA-1 is stabilized by bound mAb 24 (Dransfield et al., 1992; Hogg et al., 2002). To test how such stabilization might affect the focal zone and T cell migration, we exposed migrating T cells to mAb 24 over a longer time period. The density of ICAM-1 within the focal zone increased (Fig. 5 C) and, when the rate of recruitment of ICAM-1 was quantified, it was found to increase in a linear manner ($r^2 = 0.9344$; Fig. 5 D). Prolonged incubation with mAb 24 beyond 120 s caused extension of the focal zone and failure of trailing edge detachment resulting in T cell elongation (Fig. 5 E) and loss of motility (not depicted). These findings suggest that high affinity clustered LFA-1 is restricted to the focal zone in migrating T cells and that LFA-1 is converted from high to low affinity form between the focal zone and the uropod. When the turnover of LFA-1–ICAM-1 is prevented by mAb 24, this barrier disappears and migration is retarded.
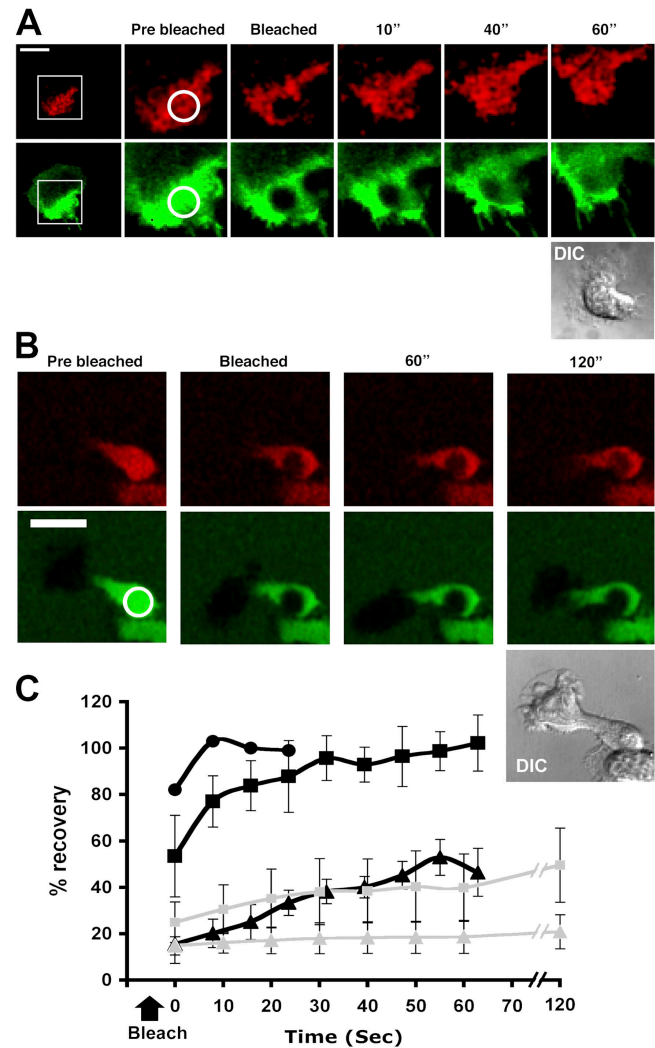
Figure 6. **The mobility of total and high affinity LFA-1 within the focal zone.** (A) T cells were labeled with nonfunction blocking Alexa 488–conjugated anti–LFA-1 Fab' and allowed to attach and migrate on the ICAM-1 bilayer. An area within the zone of ICAM-1 was photobleached (circled; 2 μm diam) at time 0 and fluorescence recovery was recorded over 60 s. LFA-1 (green) showed partial recovery, whereas ICAM-1 (red) rapidly recovers and is complete by 30 s. The boxed region shows the T cell region enlarged in subsequent images. (B) T cells were allowed to attach and migrate on the ICAM-1 bilayer in the presence of Alexa 488–labeled mAb 24 Fab'. An area within the zone of ICAM-1 was photobleached at time 0 and fluorescence recovery was recorded over 120 s. High affinity LFA-1 (green) showed no recovery, whereas ICAM-1 (red) partially recovers by 120 s. (C) Quantification of the recovery in the focal zone of LFA-1 (closed triangle), high affinity LFA-1 (+ mAb 24) (shaded triangle), ICAM-1 (closed square), ICAM-1 (+ mAb 24) (shaded square), and ICAM-1 within the bilayer as a control (closed circle) ($n = 8$; ±SD). All images were taken with a 63× oil immersion objective. Bars, 10 μm.

LFA-1 dynamics within the focal zone

The build-up of LFA-1 in the focal zone suggested that the mobility of LFA-1 must be regulated, probably by cytoskeletal attachment. To test this idea further, we compared the dynamics of total LFA-1 and high affinity (mAb 24 bound) LFA-1 by FRAP of an area within the focal zone. Fluorescent LFA-1 moved into the bleached region but did not completely replace bleached LFA-1 during the course of the experiment (Fig. 6, A and C, green). Locking LFA-1 into the high affinity conforma-

Table I. Mobility of LFA-1 on migrating T cells

Substrate	Bleached area	Mobile fraction (% ± SEM)	Diffusion coefficient (cm²/s × 10⁻¹⁰ ± SD)
PLL	Membrane	53.5 ± 2.0	3.1 ± 0.5
ICAM-1	Focal zone	38.8 ± 1.8	2.6 ± 0.4
ICAM-1	Focal zone + mAb 24	6.2 ± 0.6	–[a]
ICAM-1	Uropod	36.1 ± 2.8	2.7 ± 0.5
ICAM-1	Uropod + mAb 24	49.7 ± 3.5	3.3 ± 0.2

T cells were labeled with nonfunction-blocking Alexa 488–conjugated anti–LFA-1 Fab′ and allowed to attach to PLL or migrate on ICAM-1 in the presence or absence of 10 μg/ml mAb 24. Photobleaching (2 or 3 μm diam) was performed on randomly selected areas on the membrane of PLL-attached T cells that represented LFA-1 in a ligand-free situation (membrane) or within the membrane subregions (focal zone or uropod) of T cells migrating on ICAM-1, which represented LFA-1 in a ligand-exposed situation. Fluorescence recovery was recorded over 60 s (n = 14–22).
[a]The lack of recovery of LFA-1 in the focal zone in the presence of mAb 24 prevented calculation of a diffusion coefficient.

tion with mAb 24 resulted in the further inhibition of membrane mobility in the focal zone as seen by the lack of recovery in fluorescence (Fig. 6, B and C, green). Quantification of the mobile fraction of LFA-1 located in the focal zone shows it to be reduced from 38.8 to 6.2%, indicating that high affinity LFA-1 is under cytoskeletal constraint. These results provide evidence of a dynamic relationship between high affinity LFA-1 linked to the cytoskeleton and a mobile fraction of LFA-1 within the zone (Table I).

We next measured the recovery of ICAM-1 binding in the focal zone +/− mAb 24 as a direct indicator of ligand binding capability of LFA-1. ICAM-1 recovers completely after photobleaching, demonstrating rapid recovery of ligand binding (Fig. 6, A and C, red). However, in the presence of mAb 24, recovery is reduced (Fig. 6, B and C, red). This shows that when LFA-1 is locked in the high affinity state, turnover of LFA-1–ICAM-1 binding is prevented suggesting that a dynamic equilibrium between affinity states must exist in the focal zone.

We next compared the proportion of mobile LFA-1 in the focal zone to other areas of the cell, particularly the uropod with its high level of LFA-1. When FRAP was performed on the uropod, the resident LFA-1 showed a comparable proportion of mobile LFA-1 to the focal zone but, importantly, no decrease in the mobile fraction after mAb 24 addition (Table I). Similar results were obtained for the lamellipodial region (unpublished data) and also for nonmigrating T cells attached to poly-L-lysine (PLL). Thus, high affinity LFA-1 on the migrating T cell is restricted to the focal zone. As the immobile fraction located in the uropod is not affected by mAb 24, it must represent a form of LFA-1 that is not in the high affinity conformation but also linked to the cytoskeleton. Future work will further address this issue. It is of interest to note that the diffusion coefficients of mobile LFA-1 are similar in the focal zone and uropod and independent of mAb 24 (Table I).

Connection between the focal zone and talin

Because the FRAP studies indicated that high affinity LFA-1 was not freely mobile in the membrane, we explored which cy-

toskeletal proteins might be associated with LFA-1 in the focal zone. Talin was considered to be a prime candidate, as it has previously been reported to bind directly to β2 integrin (Pavalko and LaRoche, 1993; Sampath et al., 1998) and to activate LFA-1 (Kim et al., 2003). The T cell line HSB-2 stably expressing the GFP-tagged β2 subunit of LFA-1 (β2-GFP) was plated onto ICAM-1 and allowed to migrate before fixation and counterstaining for talin. The distribution of β2-GFP was in accordance with the LFA-1 pattern reported in Fig. 3 for T cells migrating on ICAM-1 (Fig. 7 A). With regard to talin, the highest level localized to the focal zone (Fig. 7 A, a vs. b; and Fig. 7 A, d) and a composite image in the y-z axis showed it to be concentrated at the interface of LFA-1 interacting with ICAM-1 (Fig. 7 A, c and e). This was in contrast to other intracellular proteins involved in T cell polarization and migration such as the uropod-located ezrin and the lamellipodia-associated Rac-1 and Vav-1 (Fig. S2). Therefore, talin is specifically associated with the focal zone where high affinity LFA-1 is located. To further characterize this association, we transiently transfected HSB-2 cells with a talin head domain–GFP construct (Tremuth et al., 2004) and allowed the cells to migrate on the ICAM-1–embedded lipid bilayer. Talin head–GFP localized to the region of concentrated ICAM-1 corresponding to the focal zone (Fig. 7 B and Fig. S3).

Although talin localizes to the mid-cell region of the migrating T cell, this does not prove that talin is actively involved in the formation and stabilization of the focal zone. To address this issue, talin knock-down was performed and the effect on migration observed. The use of a single siRNA construct reduced talin by ∼65% after 72 h compared with cells treated with a control siRNA construct (Fig. 7 D). The ability of T cells to concentrate ICAM-1 and form a focal zone after talin knock-down was assessed on an ICAM-1–incorporated lipid bilayer (Fig. 7 C). Knocking down talin resulted in a significant (P < 0.001) reduction in ICAM-1 accumulation in the focal zone (2.3-fold decrease) compared with control siRNA-treated cells. The importance of an intact focal zone comprising LFA-1 linked to the cytoskeleton via talin was further demonstrated by a migration assay on ICAM-1. Talin knock-down resulted in a 57% loss in LFA-1–mediated T cell speed compared with control cells (Fig. 7 E). These T cells also showed a reduced ability to translocate, as only 10% of attached cells were able to migrate further than 20 μm from their original position in 20 min compared with 37.5% of control cells (Fig. 7 F). Therefore, the decrease in talin resulted in defective T cell locomotion due to diminished focal zone formation.

To further define a functional link between talin and LFA-1, we sought to disrupt talin binding using an 18-polymer peptide corresponding to the PIPKIγ binding site for talin compared with a control peptide containing a tryptophan[647] to alanine mutation (Fig. S4, available at http://www.jcb.org/cgi/content/full/jcb.200412032/DC1; Morgan et al., 2004). Primary T cells that were exposed to the PIPKIγ peptide displayed a 61% reduction in migratory speed compared with a 1% reduction when the control peptide was added (Fig. 7 G). We asked whether focal zone stability was dependent on a link between talin and LFA-1. T cells were allowed to migrate on
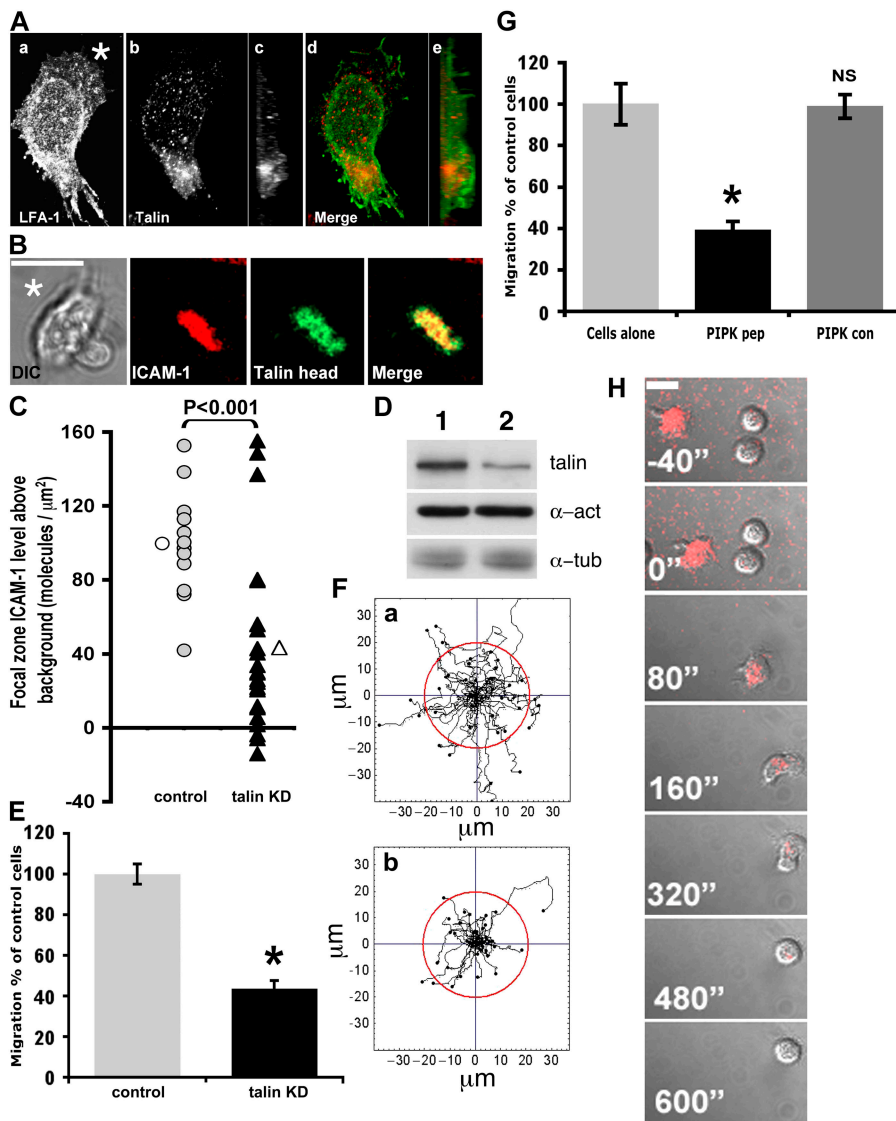
Figure 7. **LFA-1 and talin colocalize to the focal zone, and effects on migration upon disruption of talin stability.** (A) The HSB-2 T cell line expressing β2-GFP migrating on ICAM-1 was fixed and stained for talin. (a) Confocal image of LFA-1-GFP distribution was taken at the coverslip level (asterisk denotes leading edge). (b) An x-y projection of endogenous talin. (c) A y-z projection stained for talin. (d) An x-y projection of the merged LFA-1 (green) and talin (red) images. (e) A y-z projection of the merged LFA-1 (green) and talin (red) images. (B) The HSB-2 T cell line transfected with talin head domain–GFP (green) and allowed to migrate on ICAM-1 (red) after the addition of mAb 24. The merged image shows the colocalization of talin with concentrated ICAM-1. All images were taken with a 63× oil immersion objective. Bars, 10 μm. (C) HSB-2 cells were transfected with siRNA, and the effects on focal zone formation were calculated for talin knock-down and a control sequence. The knock-down of talin had a significant (P < 0.001) reduction in ICAM-1 accumulation in the focal zone compared with control siRNA (n = 14 control [shaded circle], mean value [open circle]; n = 24 talin [closed triangle], mean value [open triangle]). (D) Western blot analysis of talin knock-down in HSB-2 control cells (lane 1) and talin knock-down cells (lane 2) probed for talin and two control cytoskeletal proteins (α-actinin and α-tubulin). (E) T cell ICAM-1 migration assay using talin knock-down cells (n = 40) compared with control cells (n = 40). Results are expressed as a percentage of control cells ± SEM (*, P < 0.05). (F) The migratory tracks produced by T cells migrating on ICAM-1. a, control cells (n = 40); b, talin knock-down cells (n = 40). The red circle indicates a distance of 20 μm from the original position. (G) T cell activated with 5 mM MgCl₂ were plated onto immobilized ICAM-1 in the presence of 30 μg/ml PIPKIγ peptide (n = 60), PIPKIγ control (n = 54), or untreated (n = 26) and tracked for 20 min. Results are expressed as a percentage of untreated cells ± SEM (*, P < 0.05). (H) The effect on T cell migration and focal zone formation in the presence of the PIPKIγ peptide. T cells were allowed to attach and migrate on ICAM-1 lipid bilayers in the presence of 5 mM Mg²⁺. The PIPKIγ peptide (30 μg/ml) was injected (0 s) and the T cell followed for 600 s. The image represents the DIC image overlaid with the ICAM-1 (red) distribution.

an ICAM-1–expressing lipid bilayer before injection of the PIPKIγ peptide. Migration was inhibited and this coincided with the loss of the focal zone as determined by ICAM-1 accumulation (Fig. 7 H and Video 4, available at http://www.jcb.org/cgi/content/full/jcb.200412032/DC1). The control peptide had no effect on either migratory speed or focal zone stability (Fig. S4). In summary, the findings indicate that LFA-1 is associated with talin within the focal zone and talin provides a critical linkage into the cytoskeletal machinery, permitting stabilization of LFA-1–ICAM-1 in the focal zone and rapid T cell migration.

Discussion

In this study we have identified the lamellipodia, mid-cell, and uropod as three distinct regions of LFA-1 distribution and activity on migrating T cells. We have focused particularly on

a mid-cell region of high ICAM-1 binding activity that we have termed the focal zone, which contains high affinity, clustered LFA-1. Talin expression and localization are critical for focal zone formation, stability, and T cell migration as interference with the talin–integrin link inhibits these processes. The results suggest that talin provides LFA-1 with a critical linkage to the cytoskeleton. The zone of high affinity LFA-1 is observed on T cells migrating on purified ICAM-1, as well as on target cell membranes where other receptor binding pairs may also be engaged. In this study, we have concentrated on migration induced by direct stimulation of LFA-1, but a similar focal zone pattern is displayed for T cell migration initiated by chemokine stimulation. Thus, this arrangement of a mid-cell zone of active LFA-1 is a feature of T cell migration stimulated in several ways. As the focal zone is located between the lamellipodia and the uropod, it has the potential to form an adhesive platform supporting the multi-

ple short-lived interactions made by the lamellipodia as the T cell scans target cell surfaces while migrating.

Formation of a concentrated zone of active LFA-1 on the T cell suggests a very different process of integrin-mediated migration compared with well-studied constitutively adherent cells. The motility of cells such as the fibroblast involves coordination of multiple, individual adhesions. Stationary FCs at the leading edge mature into more rapidly turning over FAs in conjunction with stable FAs at the trailing edge (Webb et al., 2002; Wehrle-Haller and Imhof, 2002). A major difference is in the motility of these cells, as T cells migrate both in vitro and in vivo at speeds 100 times faster than fibroblasts (Abercrombie, 1961; Hogg et al., 2003). However, studies on heart fibroblast and neural crest cells report migratory speeds more closely matched with T cells. The neural crest cell can migrate at speeds up to 2 μm/min, which is 20 times faster than FA/FC-mediated motility and only 5 times slower than T cells (Strachan and Condic, 2003). This increased speed coincides with a more even distribution of integrin and limited formation of FA/FC (Duband et al., 1988). Further information about these cells with regard to membrane interaction with ligand and affinity status of the integrins could identify a link with T cells with regard to their mechanism of migration and potentially help to define general features required for rapid motility.

The fact that mAb 24, which locks LFA-1 into the high affinity form, locates solely to the focal zone and promotes an increase in stable cytoskeletally linked LFA-1–ICAM-1 couples indicates that there is turnover of high affinity LFA-1 binding to ICAM-1 in this region of the cell. The FRAP experiments are also revealing in that they show differences in ICAM-1 binding and LFA-1 dynamics within the focal zone. Bleached ICAM-1 is replaced more quickly than LFA-1, suggesting that LFA-1 already within the zone LFA-1 exists in a dynamic equilibrium of lower and higher affinity states and is capable of binding fresh ligand. This interpretation is further supported by the finding that stabilizing high affinity LFA-1 with mAb 24 inhibits ICAM-1 exchange. As mAb 24 also substantially reduces the proportion of mobile LFA-1 (from 39 to 6%), the implication is that it is the mobile receptors in the zone that initiate new ligand binding and cytoskeletal attachment maintaining the focal zone in constant position as the T cell migrates. It is of interest that the lateral diffusion coefficients for the mobile fractions of LFA-1 were invariant and similar to rates previously calculated for LFA-1 and integrins on several other types of cell surfaces (Duband et al., 1988; Kucik et al., 1996).

Two distinct regions demonstrate ICAM-1 binding on a migrating T cell. In addition to the focal zone, which accounts for ~20% of the total contact area, there is widespread LFA-1–ICAM-1 interaction as detected by IRM at the leading edge. This second region comprises the remaining 80% of ICAM-1 contact. The LFA-1 in this region has few distinguishing features such as apparent clustering or high affinity status. A possibility is that an "intermediate" binding conformation of LFA-1 is expressed in this part of the cell (Shimaoka et al., 2003), potentially permitting easy make/break attachments of the forward projecting lamellipodia. For the T cell, this arrangement provides it with the ability to remain firmly attached via the focal zone, whereas the lamellipodia scans the target cells surface for antigenic peptides or explores potential exit points on an endothelial monolayer. This organization of LFA-1 activities contrasts with migrating endothelial cells that display high affinity αvβ3 at the leading edge (Kiosses et al., 2001). Such an arrangement in slower moving cells permits firm attachment to substrate along the leading edge of the migrating cell as well as at the rear as befits a cell requiring firm contact with its surroundings.

The uropod is a distinctive region projecting above the ligand interface at the trailing edge of the T cell and LFA-1 located in this region is inactive in terms of ICAM-1 binding. When LFA-1 is locked in the high affinity form using mAb 24, LFA-1–ICAM-1 binding dramatically increases in the focal zone itself and by its extension decreases the distinction between zone and uropod. The outcome is that the trailing edge becomes firmly attached, resulting in diminished speed. For T cells, speed of migration also decreases when there is a firmly attached trailing edge as a consequence of inhibition of RhoA or ROCK (Smith et al., 2003). It is tempting to speculate that switching LFA-1 to the low affinity conformation within the focal zone and detachment of the trailing edge could be under the control of RhoA/ROCK, and future work will address this question.

An additional feature of the uropod is that it contains the highest levels of LFA-1 on the migrating T cell. In this context, it is interesting that two recent papers describe, for T cells that are polarized in suspension, that the highest levels of LFA-1 are located at the front of the cell (Katagiri et al., 2003; Lee et al., 2004). We observe in this study that the T cell becomes polarized as it attaches to ICAM-1 and redistributes LFA-1 from a uniform pattern to one of concentrated LFA-1 toward the rear of the cell. This nonuniform arrangement of LFA-1 is also observed when T cells are migrating on ICAM-1 toward a chemotactic gradient. Therefore, the implication is that the presence of ICAM-1 and the ability of LFA-1 to engage with its ligand results in a redistribution from the leading edge to the mid-cell and uropod.

Maximal T cell migration in vitro correlates with the focal zone and there is a considerable reduction in speed when the zone fails to form at low ICAM-1 densities or when LFA-1 becomes locked in the high affinity conformation resulting in focal zone elongation. Furthermore, there is a direct correlation between the amount of ICAM-1 in the bilayer and the density of ICAM-1 in the focal zone, whereas the speed of migration and focal zone size is unaffected. Thus, a critical threshold level of ICAM-1 binding must be achieved in order for the mature zone to form, and further increases in ICAM-1 levels have little effect on migration. The relative lack of dependence on ICAM-1 concentrations would allow T cells to migrate within lymph nodes and inflamed tissue sites displaying varying ICAM-1 levels.

This threshold effect with regard to ICAM-1 levels and zone formation could be due to factors such as availability and abundance of appropriate cytoskeletal proteins imposing a constraint on the rate of migration. A protein with which LFA-1 has been closely associated is the cytoskeletal linker talin

(Kupfer and Singer, 1989; Monks et al., 1998). Here, we show that LFA-1 within the focal zone of the migrating T cell is associated with talin. This is in keeping with studies showing that the talin FERM domain contains an integrin binding motif that recognizes the integrin β1, β2, and β3 subunit and induces conformational change (Calderwood et al., 1999; Garcia-Alvarez et al., 2003; Kim et al., 2003; Tadokoro et al., 2003). The FERM domain is located in the talin head region and a talin head–GFP fusion protein, expressed in T cells, localized to the focal zone during migration on ICAM-1. Additional evidence for the involvement of talin in LFA-1–mediated T cell migration was provided by knocking down talin expression by siRNA. Reduced talin levels resulted in both a failure in focal zone formation and a significant ($P < 0.05$) decrease in migration on ICAM-1. Furthermore, we have interfered with the integrin talin link using a PIPKIγ peptide that contains a binding site for the FERM domain of talin overlapping the integrin binding site (Barsukov et al., 2003). T cells exposed to the PIPKIγ peptide show a reduction in migration and loss of the focal zone, indicating that LFA-1 and talin together play a pivotal role in focal zone stability that is required for migration. Together the evidence supports the idea that the talin FERM domain and the LFA-1 β2 cytoplasmic tail physically interact as previously shown (Kim et al., 2003). This interaction is restricted in location and results in the stabilization of the focal zone, permitting LFA-1–mediated T cell migration. It is also of interest that the uropod, which expresses a high level of inactive LFA-1, shows no talin colocalization. Therefore, lack of talin binding to integrin may be associated with a low affinity conformation. Further investigation of this possibility is needed.

In summary, migrating T cells need to attach and detach rapidly to exit from the circulation into tissue sites and to make short-lived contacts with target cells. The identification of a concentrated zone of active LFA-1 has revealed how T cells have optimized a structure enabling rapid migration and dynamic directional alterations without the loss of cellular attachment. We propose that this adaptation is critical for the ability of T cells to function effectively as migratory cells in the immune response.

Materials and methods

Antibodies and reagents
The following mAbs were used in this study: nonfunction blocking CD11a mAb YTH81.5 (a gift from H. Waldman, University of Oxford, Cambridge, UK); anti-CD11a mAb 38 and β2 integrin activation reporter mAb 24 (Dransfield et al., 1992; Hogg et al., 2002) prepared in house; anti-talin mAb 8d4 (Sigma-Aldrich). AlexaFluor-488 fluorochrome labeling kit was purchased from Molecular Probes. Fab' fragments, generated from mouse mAb 24 and rat mAb YTH81.5, were labeled with Alexa-Fluor-488.

Cells and cell transfections
Peripheral blood mononuclear cells were prepared from single donor leukocyte buffy coats (National Blood Transfusion Service) and T cells expanded in culture as previously described (Smith et al., 2003). PIPKIγ and control peptide were linked via a disulfide bridge to antennapedia (Fig. S4). Primary T cells were allowed to attach and migrate on ICAM-1 followed by the addition of the peptide to a final concentration of 30 μg/ml.

The HSB-2 T cell line was maintained in RPMI 1640/10% FCS before transfection by electroporation with GFP-tagged human talin head domain (residues 1–433; Tremuth et al., 2004). Alternatively, HSB-2 cells were stably transfected with the GFP-tagged β2 subunit of LFA-1 and were maintained in RPMI 1640/10% FCS with 500 μg/ml G418. HSB2 cells were washed twice in OptiMEM + GlutaMAX (GIBCO BRL) and resuspended to a final cell concentration of 4×10^7 cells/ml. Predesigned siRNA against human talin 1 (ID 5552) (Ambion) or control siRNA (ID 4611G) was added at 400 nmol to 2×10^7 cells and electroporated at 960 μFD /260 V. The cells were then added to prewarmed RPMI 1640/10% FCS and maintained for 48 h at 37°C + 5% CO_2. The efficiency of talin knock-down was evaluated by Western blot analysis and quantification as done by NIH image 1.63 software.

HUVECs (passage 2) were maintained in Bulletkit (Clonetics). COS-7 cells were obtained from London Research Institute Cell Services Department and maintained in RPMI 1640 before transfection by electroporation with ICAM-1-GFP (Wulfing et al., 1998; a gift from M. Davis, Howard Hughes Medical Institute, Stanford, CA).

Planar lipid bilayers
The GPI-linked ICAM-1 protein was generated, purified, and labeled with AlexaFluor-543 as previously described (Bromley et al., 2001; Carrasco et al., 2004). Planar lipid bilayers were formed as previously described (Carrasco et al., 2004). AlexaFluor-543 GPI-linked ICAM-1–containing liposomes were mixed with 1,2-dioleoyl-phosphatidylcholine lipids (Avanti Polar Lipids, Inc.) at different ratios to achieve the required molecular densities. The FCS2 flow chambers (Bioptechs) were blocked with PBS containing 2% BSA. T cells (2×10^6 cells/ml) in HBSS containing 20 mM Hepes and 5 mM $MgCl_2$ were injected into the warmed chamber (37°C) and, after injection, the flow was stopped. In some experiments, T cells were either preincubated with the labeled YTH81.5 Fab' or, alternatively, labeled or unlabeled mAb 24 Fab' was injected onto bilayer-attached T cells. Confocal fluorescence and differential interference contrast (DIC) images were obtained simultaneously at specified time intervals. The contact of T cells with the lipid bilayer was visualized by IRM. Images were acquired on an inverted microscope (model Axiovert LSM-510-META; Carl Zeiss MicroImaging, Inc.) with a 63× oil immersion objective and analyzed using LSM-510 (Carl Zeiss MicroImaging, Inc.) and AQM[2001] Kinetic Acquisition Manager (Kinetic Imaging Ltd.) software. ICAM-1 quantification was performed as previously described (Carrasco et al., 2004).

FRAP
T cells were added to bilayers containing 175 Alexa 543–labeled ICAM-1 molecules/μm^2 in the presence of 10 μg/ml Alexa 488–labeled nonfunctional blocking anti–LFA-1 Fab' (YTH81.5) or Alexa 488–labeled mAb 24 and allowed to attach and migrate. The selected fluorescent region (5–25 μm^2) was exposed to a pulse of an Argon laser (488 nm) and the He/Ne laser (543 nm) to irreversibly bleach the fluorophores. Images were acquired to follow the recovery process in the bleached area. The fluorescence signal recovered at a given time point was obtained by dividing the fluorescent signal at that time point by the fluorescent signal at time 0 in the selected area. The mobile fraction was identified as those receptors displaying recovery after photobleaching and expressed as a percentage: (final signal − bleached signal)/(initial signal − bleached signal) × 100%. Three separate membrane locations were investigated: the focal zone and uropod on T cells migrating on immobilized ICAM-1 and the plasma membrane of T cells adhered to 0.01% PLL in the absence of ICAM-1. The diffusion coefficients for LFA-1 were calculated as previously described (Axelrod et al., 1976).

Confocal microscopy
ICAM-1Fc–coated coverslips were prepared as previously described (Smith et al., 2003). β2-GFP–expressing HSB-2 cells were allowed to adhere and migrate for 20 min at 37°C and unbound cells were washed off. After fixation, cells were permeabilized with 0.1% Triton X-100 and labeled with anti-talin (1:200; Sigma-Aldrich) followed by Alexa 532 anti–mouse IgG (H+L chain) (Cambridge Bioscience). COS-7 cells were transfected with ICAM-1-GFP and grown on 13-mm coverslips. The coverslips were washed with HBSS/20 mM Hepes/3 mM $MgCl_2$. 2×10^5 T cells were added and allowed to adhere and migrate for 20 min at 37°C, and unbound cells were washed off. After fixation, cells were permeabilized with 0.1% Triton X-100 and labeled with Alexa 546 YTH81.5. Confocal images were collected using an inverted microscope in the x-y plane at 1-μm intervals. Three-dimensional reconstruction was performed using LSM-510 software (Carl Zeiss MicroImaging, Inc.).

Video microscopy
For video microscopy, 35-mm glass bottom microwell dishes (MatTek Corp.) were coated overnight with 3 μg/ml ICAM-1-Fc, and then blocked

with 2% BSA in PBS. T cells (4×10^5/ml in HBSS/20 mM Hepes buffer) were added and allowed to settle for 10 min at 37°C, and nonattached cells were removed by gentle washing. Images were taken using a microscope (model Diaphot 300; Nikon), 40× lens, and AQM[2001] Kinetic Acquisition Manager software. Cells were tracked at 5-s intervals using Motion Analysis software (Kinetic Imaging Ltd.) and the data were analyzed using a Mathematica notebook (Wolfram Research Inc.) developed by D. Zicha (Cancer Research UK, London, UK). Migration speeds were expressed as a percentage of control cells over 20 min ± SEM. Statistical analysis was performed using ANOVA test.

Online supplemental material

Fig. S1 shows LFA-1 surface distribution on a T cell migrating in an SDF-1 chemotactic gradient. Fig. S2 shows membrane polarity markers on migrating T cells. Fig. S3 shows a talin head–GFP–expressing T cell and an intensity profile of mAb 24 and ICAM-1. Fig. S4 shows the sequence for the PIPKIγ plus control peptide and the effect of the control peptide on the focal zone. Video 1 shows LFA-1–labeled T cells migrating on endothelial cells. Video 2 shows the LFA-1 focal zone on migrating T cells. Video 3 shows the migration of an anti–LFA-1–labeled T cell on ICAM-1. Video 4 shows the effect of the PIPKIγ peptide on focal zone stability. Online supplemental material is available at http://www.jcb.org/cgi/content/full/jcb.200412032/DC1.

References

Abercrombie, M. 1961. The basis of locomotory behaviour of fibroblasts. *Exp. Cell Res.* Suppl. 8:188–198.

Axelrod, D., D.E. Koppel, J. Schlessinger, E. Elson, and W.W. Webb. 1976. Mobility measurement by analysis of fluorescence photobleaching recovery kinetics. *Biophys. J.* 16:1055–1069.

Ballestrem, C., B. Hinz, B.A. Imhof, and B. Wehrle-Haller. 2001. Marching at the front and dragging behind: differential αVβ3-integrin turnover regulates focal adhesion behavior. *J. Cell Biol.* 155:1319–1332.

Barsukov, I.L., A. Prescot, N. Bate, B. Patel, D.N. Floyd, N. Bhanji, C.R. Bagshaw, K. Letinic, G. Di Paolo, P. De Camilli, et al. 2003. Phosphatidylinositol phosphate kinase type 1gamma and beta1-integrin cytoplasmic domain bind to the same region in the talin FERM domain. *J. Biol. Chem.* 278:31202–31209.

Bromley, S.K., A. Iaboni, S.J. Davis, A. Whitty, J.M. Green, A.S. Shaw, A. Weiss, and M.L. Dustin. 2001. The immunological synapse and CD28-CD80 interactions. *Nat. Immunol.* 2:1159–1166.

Calderwood, D.A., and M.H. Ginsberg. 2003. Talin forges the links between integrins and actin. *Nat. Cell Biol.* 5:694–697.

Calderwood, D.A., R. Zent, R. Grant, D. Jasper, G. Rees, R.O. Hynes, and M.H. Ginsberg. 1999. The talin head domain binds to integrin beta subunit cytoplasmic tails and regulates integrin activation. *J. Biol. Chem.* 274:28071–28074.

Carrasco, Y.R., S.J. Fleire, T. Cameron, M.L. Dustin, and F.D. Batista. 2004. LFA-1/ICAM-1 interaction lowers the threshold of B cell activation by facilitating B cell adhesion and synapse formation. *Immunity.* 20:589–599.

Critchley, D.R. 2000. Focal adhesions-the cytoskeletal connection. *Curr. Opin. Cell Biol.* 12:133–139.

Di Paolo, G., L. Pellegrini, K. Letinic, G. Cestra, R. Zoncu, S. Voronov, S. Chang, J. Guo, M.R. Wenk, and P. De Camilli. 2002. Recruitment and regulation of phosphatidylinositol phosphate kinase type 1 gamma by the FERM domain of talin. *Nature.* 420:85–89.

Dransfield, I., and N. Hogg. 1989. Regulated expression of Mg^{2+} binding epitope on leukocyte integrin alpha subunits. *EMBO J.* 8:3759–3765.

Dransfield, I., C. Cabanas, J. Barrett, and N. Hogg. 1992. Interaction of leukocyte integrins with ligand is necessary but not sufficient for function. *J. Cell Biol.* 116:1527–1535.

Duband, J.L., G.H. Nuckolls, A. Ishihara, T. Hasegawa, K.M. Yamada, J.P. Thiery, and K. Jacobson. 1988. Fibronectin receptor exhibits high lateral mobility in embryonic locomoting cells but is immobile in focal contacts and fibrillar streaks in stationary cells. *J. Cell Biol.* 107:1385–1396.

Dunlevy, J.R., and J.R. Couchman. 1993. Controlled induction of focal adhesion disassembly and migration in primary fibroblasts. *J. Cell Sci.* 105:489–500.

Dustin, M.L., S.K. Bromley, Z. Kan, D.A. Peterson, and E.R. Unanue. 1997. Antigen receptor engagement delivers a stop signal to migrating T lymphocytes. *Proc. Natl. Acad. Sci. USA.* 94:3909–3913.

Garcia-Alvarez, B., J.M. de Pereda, D.A. Calderwood, T.S. Ulmer, D.R. Critchley, I.D. Campbell, M.H. Ginsberg, and R.C. Liddington. 2003. Structural determinants of integrin recognition by talin. *Mol. Cell.* 11:49–58.

Hogg, N., R. Henderson, B. Leitinger, A. McDowall, J. Porter, and P. Stanley. 2002. Mechanisms contributing to the activity of integrins on leukocytes. *Immunol. Rev.* 186:164–171.

Hogg, N., M. Laschinger, K. Giles, and A. McDowall. 2003. T-cell integrins: more than just sticking points. *J. Cell Sci.* 116:4695–4705.

Jacobelli, J., S.A. Chmura, D.B. Buxton, M.M. Davis, and M.F. Krummel. 2004. A single class II myosin modulates T cell motility and stopping, but not synapse formation. *Nat. Immunol.* 5:531–538.

Katagiri, K., A. Maeda, M. Shimonaka, and T. Kinashi. 2003. RAPL, a Rap1-binding molecule that mediates Rap1-induced adhesion through spatial regulation of LFA-1. *Nat. Immunol.* 4:741–748.

Kim, M., C.V. Carman, and T.A. Springer. 2003. Bidirectional transmembrane signaling by cytoplasmic domain separation in integrins. *Science.* 301:1720–1725.

Kiosses, W.B., S.J. Shattil, N. Pampori, and M.A. Schwartz. 2001. Rac recruits high-affinity integrin alphavbeta3 to lamellipodia in endothelial cell migration. *Nat. Cell Biol.* 3:316–320.

Kucik, D.F., M.L. Dustin, J.M. Miller, and E.J. Brown. 1996. Adhesion-activating phorbol ester increases the mobility of leukocyte integrin LFA-1 in cultured lymphocytes. *J. Clin. Invest.* 97:2139–2144.

Kupfer, A., and S.J. Singer. 1989. The specific interaction of helper T cells and antigen-presenting B cells. IV. Membrane and cytoskeletal reorganizations in the bound T cell as a function of antigen dose. *J. Exp. Med.* 170:1697–1713.

Laukaitis, C.M., D.J. Webb, K. Donais, and A.F. Horwitz. 2001. Differential dynamics of α5 integrin, paxillin, and α-actinin during formation and disassembly of adhesions in migrating cells. *J. Cell Biol.* 153:1427–1440.

Lee, J.H., T. Katakai, T. Hara, H. Gonda, M. Sugai, and A. Shimizu. 2004. Roles of p-ERM and Rho–ROCK signaling in lymphocyte polarity and uropod formation. *J. Cell Biol.* 167:327–337.

Ling, K., R.L. Doughman, A.J. Firestone, M.W. Bunce, and R.A. Anderson. 2002. Type I gamma phosphatidylinositol phosphate kinase targets and regulates focal adhesions. *Nature.* 420:89–93.

Liu, S., D.A. Calderwood, and M.H. Ginsberg. 2000. Integrin cytoplasmic domain-binding proteins. *J. Cell Sci.* 113:3563–3571.

Mempel, T.R., S.E. Henrickson, and U.H. Von Andrian. 2004. T-cell priming by dendritic cells in lymph nodes occurs in three distinct phases. *Nature.* 427:154–159.

Miller, M.J., S.H. Wei, M.D. Cahalan, and I. Parker. 2003. Autonomous T cell trafficking examined in vivo with intravital two-photon microscopy. *Proc. Natl. Acad. Sci. USA.* 100:2604–2609.

Monks, C.R., B.A. Freiberg, H. Kupfer, N. Sciaky, and A. Kupfer. 1998. Three-dimensional segregation of supramolecular activation clusters in T cells. *Nature.* 395:82–86.

Morgan, J.R., G. Di Paolo, H. Werner, V.A. Shchedrina, M. Pypaert, V.A. Pieribone, and P. De Camilli. 2004. A role for talin in presynaptic function. *J. Cell Biol.* 167:43–50.

Nayal, A., D.J. Webb, and A.F. Horwitz. 2004. Talin: an emerging focal point of adhesion dynamics. *Curr. Opin. Cell Biol.* 16:94–98.

Pavalko, F.M., and S.M. LaRoche. 1993. Activation of human neutrophils induces an interaction between the integrin beta 2-subunit (CD18) and the actin binding protein alpha-actinin. *J. Immunol.* 151:3795–3807.

Ridley, A.J., M.A. Schwartz, K. Burridge, R.A. Firtel, M.H. Ginsberg, G. Borisy, J.T. Parsons, and A.R. Horwitz. 2003. Cell migration: integrating signals from front to back. *Science.* 302:1704–1709.

Sampath, R., P.J. Gallagher, and F.M. Pavalko. 1998. Cytoskeletal interactions with the leukocyte integrin beta2 cytoplasmic tail. Activation-dependent regulation of associations with talin and alpha-actinin. *J. Biol. Chem.* 273:33588–33594.

Shimaoka, M., T. Xiao, J.H. Liu, Y. Yang, Y. Dong, C.D. Jun, A. McCormack, R. Zhang, A. Joachimiak, J. Takagi, et al. 2003. Structures of the alpha L I domain and its complex with ICAM-1 reveal a shape-shifting pathway for integrin regulation. *Cell.* 112:99–111.

Smith, A., M. Bracke, B. Leitinger, J.C. Porter, and N. Hogg. 2003. LFA-1-induced T cell migration on ICAM-1 involves regulation of MLCK-mediated attachment and ROCK-dependent detachment. *J. Cell Sci.* 116: 3123–3133.

Strachan, L.R., and M.L. Condic. 2003. Neural crest motility and integrin regulation are distinct in cranial and trunk populations. *Dev. Biol.* 259:288–302.

Tadokoro, S., S.J. Shattil, K. Eto, V. Tai, R.C. Liddington, J.M. de Pereda, M.H. Ginsberg, and D.A. Calderwood. 2003. Talin binding to integrin beta tails: a final common step in integrin activation. *Science.* 302:103–106.

Tremuth, L., S. Kreis, C. Melchior, J. Hoebeke, P. Ronde, S. Plancon, K. Takeda, and N. Kieffer. 2004. A fluorescence cell biology approach to map the second integrin-binding site of talin to a 130-amino acid sequence within the rod domain. *J. Biol. Chem.* 279:22258–22266.

Vicente-Manzanares, M., and F. Sanchez-Madrid. 2004. Role of the cytoskeleton during leukocyte responses. *Nat. Rev. Immunol.* 4:110–122.

Webb, D.J., J.T. Parsons, and A.F. Horwitz. 2002. Adhesion assembly, disassembly and turnover in migrating cells—over and over and over again. *Nat. Cell Biol.* 4:E97–E100.

Wehrle-Haller, B., and B. Imhof. 2002. The inner lives of focal adhesions. *Trends Cell Biol.* 12:382–389.

Wulfing, C., M.D. Sjaastad, and M.M. Davis. 1998. Visualizing the dynamics of T cell activation: intracellular adhesion molecule 1 migrates rapidly to the T cell/B cell interface and acts to sustain calcium levels. *Proc. Natl. Acad. Sci. USA.* 95:6302–6307.